
BiDM: Pushing the Limit of Quantization for Diffusion Models

Xingyu Zheng¹, Xianglong Liu^{✉1}, Yichen Bian¹, Xudong Ma¹, Yulun Zhang²,
 Jiakai Wang³, Jinyang Guo¹, Haotong Qin⁴
¹Beihang University ²Shanghai Jiao Tong University
³Zhongguancun Laboratory ⁴ETH Zürich
 {zhengxingyu,xlliu,macaronlin,jinyangguo}@buaa.edu.cn
 {yichen.bian.work,yulun100}@gmail.com wangjk@zgclab.edu.cn
 haotong.qin@pbl.ee.ethz.ch

Abstract

Diffusion models (DMs) have been significantly developed and widely used in various applications due to their excellent generative qualities. However, the expensive computation and massive parameters of DMs hinder their practical use in resource-constrained scenarios. As one of the effective compression approaches, quantization allows DMs to achieve storage saving and inference acceleration by reducing bit-width while maintaining generation performance. However, as the most extreme quantization form, 1-bit binarization causes the generation performance of DMs to face severe degradation or even collapse. This paper proposes a novel method, namely **BiDM**, for fully binarizing weights and activations of DMs, pushing quantization to the 1-bit limit. From a temporal perspective, we introduce the *Timestep-friendly Binary Structure* (TBS), which uses learnable activation binarizers and cross-timestep feature connections to address the highly timestep-correlated activation features of DMs. From a spatial perspective, we propose *Space Patched Distillation* (SPD) to address the difficulty of matching binary features during distillation, focusing on the spatial locality of image generation tasks and noise estimation networks. As the first work to fully binarize DMs, the WIA1 BiDM on the LDM-4 model for LSUN-Bedrooms 256×256 achieves a remarkable FID of 22.74, significantly outperforming the current state-of-the-art general binarization methods with an FID of 59.44 and invalid generative samples, and achieves up to excellent 28.0× storage and 52.7× OPs savings.

1 Introduction

Diffusion models (DMs) [19; 50; 44; 76], as a type of generative visual model [66; 59; 68], have garnered impressive attention and applications in various fields, such as image [57; 58], speech [42; 45; 24], and video [40; 18], because of their high-quality and diverse generative capabilities. The diffusion model can generate data from random noise through up to 1000 denoising steps [19]. Although some accelerated sampling methods effectively reduce the number of steps required for generating tasks [56; 31], the expensive floating-point computation of each timestep still limits its wide application on resource-constrained scenarios. Therefore, compression of the diffusion model becomes a crucial step for its broader application, and existing compression methods mainly include quantization [30; 54; 47], distillation [53; 36; 41; 73; 11], pruning [7; 12; 14; 13], *etc.* These compression approaches aim to reduce storage and computation while preserving accuracy.

Quantization is considered a highly effective model compression technique [70; 9; 64; 21; 10], which quantizes the weights and/or activations to low-bit integers or binaries for compact storage and

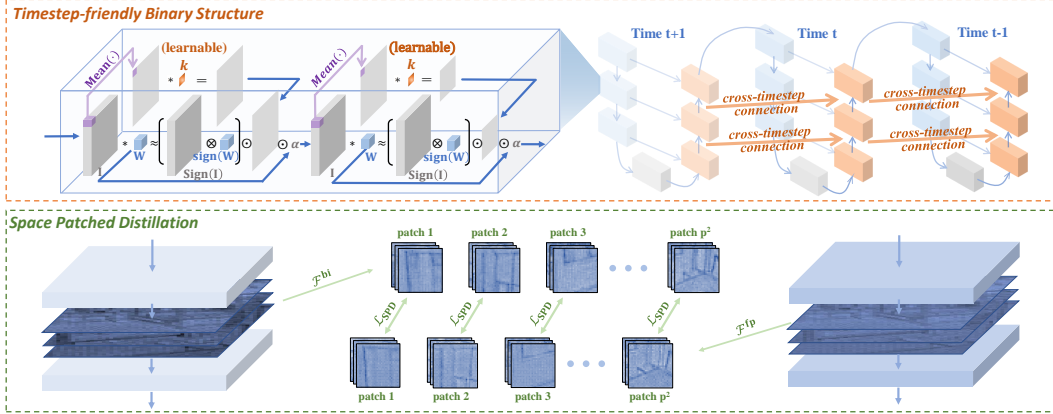


Figure 1: Overview of BiDM with *Timestep-friendly Binary Structure*, which improves DM architecture temporally, and *Space Patched Distillation*, which enhances DM optimization spatially.

efficient computation in inference. Some existing works thus apply quantization to compress DMs, aiming to compress and accelerate them while maintaining the quality of generation. Among them, 1-bit quantization, namely binarization, can achieve maximum storage savings for models and has performed well in discriminative models such as CNNs [33; 67; 65]. Furthermore, when both weights and activations are quantized to 1-bit, *e.g.*, fully binarized, efficient bitwise operations such as XNOR and bitcount can replace matrix multiplication, achieving the most efficient acceleration [74].

Some existing works have attempted to quantize DM to 1-bit [77], but their exploration mainly focuses on the weights, which are still far from full binarization. In fact, for generative models like DM, the impact of fully binarizing weights and activations is catastrophic: a) As generative models, DMs have rich intermediate representations closely related to timesteps and highly dynamic activation ranges, which are both very limited in information when binarized weights and activations are used; b) Generative models like DMs are typically required to output complete images, but the highly discrete parameter and feature space make it particularly difficult for binarized DMs to match the ground truth during training. The limited representational capacity, which is hard to match with timesteps dynamically, and the optimization difficulty of generative tasks in discrete space make it difficult for the binarized DM to converge or even collapse during the optimization process.

We propose **BiDM** to push diffusion models towards extreme compression and acceleration through complete binarization of weights and activations. It is designed to address the unique properties of DMs’ activation features, model structure, and the demands of generative tasks, overcoming the difficulties associated with complete binarization. BiDM consists of two novel techniques: *From a temporal perspective*, we observe that the activation properties of DMs are highly correlated with timesteps. We introduce the Timestep-friendly Binary Structure (TBS), which uses learnable activation binary quantizers to match the highly dynamic activation ranges of DMs and designs feature connections across timesteps to leverage the similarity of features between adjacent timesteps, thereby enhancing the representation capacity of the binary model. *From a spatial perspective*, we note the spatial locality of DMs in generative tasks and the convolution-based U-Net structure. We propose Space Patched Distillation (SPD), which introduces a full-precision model as a supervisor and uses attention-guided imitation on divided patches to focus on local features, better guiding the optimization direction of the binary diffusion model.

Extensive experiments show that compared to existing SOTA fully binarized methods, BiDM significantly improves accuracy while maintaining the same inference efficiency, surpassing all existing baselines across various evaluation metrics. Specifically, in pixel space diffusion models, BiDM is the only method that raises the IS to 5.18, close to the level of full-precision models and 0.95 higher than the best baseline method. In LDM, BiDM reduces the FID on LSUN-Bedrooms from the SOTA method’s 59.44 to an impressive 22.74, while fully benefiting from $28.0\times$ storage and $52.7\times$ OPs savings. As the first fully binarized method for diffusion models, numerous generated samples also demonstrate that BiDM is currently the only method capable of producing acceptable images with fully binarized DMs, enabling the efficient application of DMs in low-resource scenarios.

2 Related Work

Diffusion models (DMs) have demonstrated excellent generative capabilities across various tasks [19; 57; 58; 43; 42; 45; 24]. However, their large-scale model architectures and the high computational costs required for multi-step inference limit their practical applications. To address this, methods for accelerating the process at the timestep level have been widely proposed, including sampling acceleration that does not require retraining [56; 31; 34; 35] and distillation methods [53; 36; 41]. A recent method called DeepCache [38] caches high-dimensional features to avoid a lot of redundant computations and is compatible with typical sampling acceleration methods. However, these methods cannot overcome the memory bottlenecks and efficiency limits during single-step inference.

Quantization is a widely validated compression technique that compresses weights and activations from the usual 32 bits to 1-8 bits to achieve compression and acceleration [6; 78; 37; 75]. Consequently, quantization is being studied for application in diffusion models [15; 4]. These methods generally consider the unique timestep structure and spatial architecture of diffusion models, but due to the significant difficulty of quantizing generative models, most post-training quantization (PTQ) methods can only quantize models to 4 bits or more [29; 54; 22], while more accurate quantization-aware training (QAT) methods face severe performance bottlenecks below 3 bits [30; 55].

Binarization, the most extreme form of quantization, typically expresses weights and activations as ± 1 , allowing the model to achieve maximum compression and acceleration [60; 62]. In computer vision, binarization work has mainly focused on discriminative models like CNNs [49; 33; 46; 48] or ViTs [28; 16], with limited work on generative models. While ResNet VAE and Flow++ [1] have achieved complete binarization for VAEs [26], they do not offer generative performance comparable to current advanced models. Binary Latent Diffusion [61] binarized the latent space of LDMs [26] but did not improve the model’s spatial footprint or inference efficiency. The latest work, BinaryDM [50], quantized DMs to nearly W1A4, but it did not address activation quantization, leaving room for achieving full binarization and acceleration of DMs.

3 Method

3.1 Binarized Diffusion Model Baseline

Diffusion models. Given a data distribution $\mathbf{x}_0 \sim q(\mathbf{x}_0)$, the forward process generates a sequence of random variables $\mathbf{x}_t \in \{\mathbf{x}_1, \dots, \mathbf{x}_T\}$ with transition kernel $q(\mathbf{x}_t | \mathbf{x}_{t-1})$, usually Gaussian perturbation, which can be expressed as

$$q(\mathbf{x}_1, \dots, \mathbf{x}_T | \mathbf{x}_0) = \prod_{t=1}^T q(\mathbf{x}_t | \mathbf{x}_{t-1}), \quad q(\mathbf{x}_t | \mathbf{x}_{t-1}) = \mathcal{N}\left(\mathbf{x}_t; \sqrt{1 - \beta_t} \mathbf{x}_{t-1}, \beta_t \mathbf{I}\right), \quad (1)$$

where $\beta_t \in (0, 1)$ is a noise schedule. Gaussian transition kernel allows us to marginalize the joint distribution, so with $\alpha_t := 1 - \beta_t$ and $\bar{\alpha}_t := \prod_{i=1}^t \alpha_i$, we can easily obtain a sample of \mathbf{x}_t by sampling a gaussian vector $\epsilon \sim \mathcal{N}(\mathbf{0}, \mathbf{I})$ and applying the transformation $\mathbf{x}_t = \sqrt{\bar{\alpha}_t} \mathbf{x}_0 + \sqrt{1 - \bar{\alpha}_t} \epsilon$.

The reverse process aims to generate samples by removing noise, approximating the unavailable conditional distribution $q(\mathbf{x}_{t-1} | \mathbf{x}_t)$ with a learnable transition kernel $p_\theta(\mathbf{x}_{t-1} | \mathbf{x}_t)$, which can be expressed as

$$p_\theta(\mathbf{x}_{t-1} | \mathbf{x}_t) = \mathcal{N}\left(\mathbf{x}_{t-1}; \tilde{\boldsymbol{\mu}}_\theta(\mathbf{x}_t, t), \tilde{\beta}_t \mathbf{I}\right). \quad (2)$$

The mean $\tilde{\boldsymbol{\mu}}_\theta(\mathbf{x}_t, t)$ and variance $\tilde{\beta}_t$ could be derived using the reparameterization tricks in [19]:

$$\tilde{\boldsymbol{\mu}}_\theta(\mathbf{x}_t, t) = \frac{1}{\sqrt{\alpha_t}} \left(\mathbf{x}_t - \frac{1 - \alpha_t}{\sqrt{1 - \bar{\alpha}_t}} \boldsymbol{\epsilon}_\theta(\mathbf{x}_t, t) \right), \quad \tilde{\beta}_t = \frac{1 - \bar{\alpha}_{t-1}}{1 - \bar{\alpha}_t} \cdot \beta_t, \quad (3)$$

where $\boldsymbol{\epsilon}_\theta$ is a function approximation with the learnable parameter θ , which predicts ϵ given \mathbf{x}_t .

For the training of DMs, a simplified variant of the variational lower bound is usually applied as the loss function for better sample quality, which can be expressed as

$$\mathcal{L}_{\text{DM}} = \mathbb{E}_{t \sim [1, T], \mathbf{x}_0 \sim q(\mathbf{x}_0), \epsilon \sim \mathcal{N}(\mathbf{0}, \mathbf{I})} \left[\|\epsilon_t - \boldsymbol{\epsilon}_\theta(\mathbf{x}_t, t)\|^2 \right]. \quad (4)$$

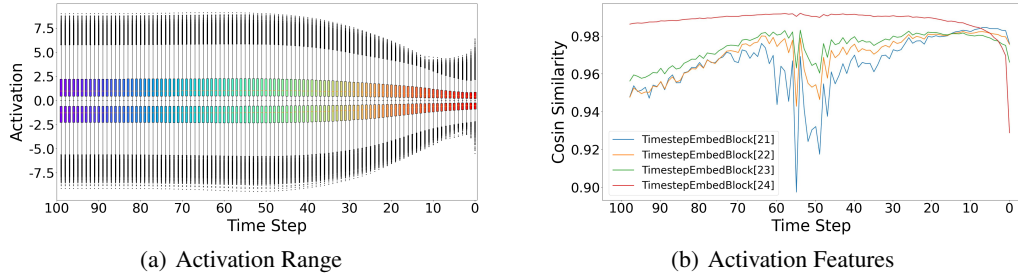


Figure 2: (a) The activation range of the 4th convolutional layer of the full-precision DDIM model on CIFAR-10 varies with the denoising timesteps. (b) The output features are similar at each step of the full-precision LDM-4 model on LSUN-Bedrooms compared to the previous step.

U-Net [51], due to its ability to fuse low-level and high-dimensional features, has become the mainstream backbone of Diffusion. The input-output blocks of U-Net can be represented as $\{D_m\}_{m=1}^d$ and $\{U_m\}_{m=1}^d$, where blocks corresponding to smaller m are more low-level. Skip connections propagate low-level information from $D_m(\cdot)$ to $U_m(\cdot)$, so the input received by U_m is expressed as:

$$\text{Concat}(D_m(\cdot), U_{m+1}(\cdot)). \quad (5)$$

Binarization. The quantization compresses and accelerates the noise estimation model by discretizing weights and activations to low bit-width. In the baseline of the binarized diffusion model, the weights \mathbf{w} are binarized to 1-bit [49; 5; 20]:

$$\mathbf{w}^{\text{bi}} = \sigma \text{sign}(\mathbf{w}) = \begin{cases} \sigma, & \text{if } \mathbf{w} \geq 0, \\ -\sigma, & \text{otherwise,} \end{cases} \quad (6)$$

where sign function confine \mathbf{w} to +1 or -1 with 0 thresholds. σ is a floating-point scalar, which is initialized as $\frac{\|\mathbf{w}\|}{n}$ (n denotes the number of weights) and learnable during training following [49; 33].

Meanwhile, activations are typically quantized by naive BNN quantizers [23; 32]:

$$\mathbf{a}^{\text{bi}} = \text{sign}(\mathbf{a}) = \begin{cases} 1, & \text{if } \mathbf{a} \geq 0, \\ -1, & \text{otherwise.} \end{cases} \quad (7)$$

When both weights and activations are quantized to 1-bit, the computations of the denoising model can be replaced by XNOR and bitcount operators, achieving significant compression and acceleration.

3.2 Timestep-friendly Binary Structure

Before delving into the detailed description of the proposed method, we summarize our observation on the properties of DMs:

Observation 1. *The activation range varies significantly across long-term timesteps, but the activation features are similar in short-term neighboring timesteps.*

Previous works, such as TDQ [55] and Q-DM [30], have commonly demonstrated that the activation distribution of DMs largely depends on denoising process, manifesting as similarities between adjacent timesteps while difference between distant ones, as shown in Figure 2(a). Therefore, applying a fixed scaling factor to activations across all timesteps can cause significant distortion in the activation range. Beyond the distribution range, Deepcache [38] highlights the substantial temporal consistency of high-dimensional features across consecutive timesteps, as shown in Figure 2(b).

These phenomena prompt us to reexamine existing binary structures. Binarization, especially the full binarization of weights and activations, results in a greater loss of activation range and precision compared to low-bit quantizations like 4-bit [50]. This makes it more challenging to generate rich activation features. Such deficiencies in activation range and output features significantly harm representation-rich generative models like DMs. Therefore, adopting binary quantizers with more

flexible activation ranges for DMs, and enhancing the model’s overall expressive power by leveraging its feature outputs, are crucial strategies for improving its generative capability after full binaryzation.

We first focus on the differences between various timesteps over the long term. Most existing activation quantizers, such as BNN [23] and Bi-Real [32], as shown in Eq. (6), directly quantize activations to $\{+1, -1\}$. This approach significantly disrupts activation features and negatively impacts the expressive power of generative models. Some improved activation binary quantizers, such as XNOR++ [2], adopt a trainable scale factor k :

$$\mathbf{a}^{\text{bi}} = K \text{sign}(\mathbf{a}) = \begin{cases} K, & \text{if } \mathbf{a} \geq 0, \\ -K, & \text{otherwise,} \end{cases} \quad (8)$$

where the form of K could be either a vector or the product of multiple vectors, but it remains a constant value during inference. Although this approach partially restores the feature expression of activations, it does not align well with diffusion models that are highly correlated with timesteps and may still lead to significant performance loss.

We turn our attention to the original XNOR, which employs dynamically computed means to construct the activation binary quantizer. Its operation for 2D convolution can be expressed as:

$$\mathbf{I} * \mathbf{W} \approx (\text{sign}(\mathbf{I}) \otimes \text{sign}(\mathbf{W})) \odot (K\alpha) = (\text{sign}(\mathbf{I}) \otimes \text{sign}(\mathbf{W})) \odot (A * k\alpha), \quad (9)$$

where $\mathbf{I} \in \mathbb{R}^{c \times w_{in} \times h_{in}}$, $\mathbf{W} \in \mathbb{R}^{c \times w \times h}$, $A = \frac{\sum \mathbf{I}_{i,:,:,1}}{c}$, $\alpha = \frac{1}{n} \|\mathbf{W}\|_{\ell_1}$. $k \in \mathbb{R}^{1 \times 1 \times w \times h}$ represents a 2D filter, where $\forall ij k_{ij} = \frac{1}{w \times h}$. $*$ and \otimes indicate convolution with and without multiplication, respectively. This approach naturally preserves the range of activation features and dynamically adapts with the input range across different timesteps. However, due to the rich expression of DM features, local activations exhibit inconsistency in range before and after passing through modules, indicating that the predetermined value of k does not effectively restore the activation representation.

Therefore, we make k adjustable and allow it to be learned during training to adaptively match the changes in the range of activations before and after. The gradient calculation process of our learnable tiny convolution k can be expressed as follows:

$$\frac{\partial \mathcal{L}}{\partial k} = \frac{\partial \mathcal{L}}{\partial (\mathbf{I} * \mathbf{W})} \frac{\partial (A * k\alpha)}{\partial k} (\text{sign}(\mathbf{I}) \otimes \text{sign}(\mathbf{W})). \quad (10)$$

Notably, making k learnable does not add any extra inference burden. The computational cost remains unchanged, allowing for efficient binary operations.

On the other hand, we focus on the similarity between adjacent timesteps. Deepcache directly extracts high-dimensional features as a cache to skip a large amount of deep computation in U-Net, achieving significant inference acceleration. This process is expressed as:

$$F_{\text{cache}}^t \leftarrow U_{m+1}^t(\cdot), \quad \text{Concat}(D_m^{t-1}(\cdot), F_{\text{cache}}^t). \quad (11)$$

However, this approach does not apply to binarized diffusion models, as the information content of each output from a binary network is very limited. For binary diffusion models, which inherently achieve significant compression and acceleration but have limited expressive power, we anticipate that the similarity of features between adjacent timesteps will enhance binary representation, thereby compensating for the representation challenges.

We construct a cross-timestep information enhancement connection to enrich the expression at the current timestep using features from the previous step. This process can be expressed as:

$$\text{Concat}(D_m^{t-1}(\cdot), (1 - \alpha_{m+1}^{t-1}) \cdot U_{m+1}^{t-1}(\cdot) + \alpha_{m+1}^{t-1} \cdot U_{m+1}^t(\cdot)), \quad (12)$$

where α_{m+1}^{t-1} is a learnable scaling factor. As shown in Figure 2(b), the similarity of high-dimensional features varies across different blocks and timesteps in DMs. Therefore, we set multiple independent α values to allow the model to adaptively learn more effectively during training.

In summary, Timestep-friendly Binary Structure (TBS) includes learnable tiny convolution applied to scaling factors after averaging the inputs and connections across timesteps. Their combined effect adapts to the changes in the activation range of diffusion models over long-range timesteps and leverages the similarity of high-dimensional features between adjacent timesteps to enhance information representation.

From the perspective of error reduction, a visualization of TBS is shown in Figure 3. First, we abstract the output of the binary DM under the baseline method as vector B^{t-1} . The mismatch in scaling factors creates a significant difference in length between it and the output vector F^{t-1} of the full-precision model. Using our proposed scaling factors and learnable tiny convolutions, B^{t-1} is expanded to L^{t-1} . L^{t-1} is closer to F^{t-1} , but there is still a directional difference from the full-precision model. The cross-timestep connection further incorporates the outputs F^t of the previous timestep, B^t , and L^t . The high-dimensional feature similarity between adjacent timesteps means the gap between F^{t-1} and F^t

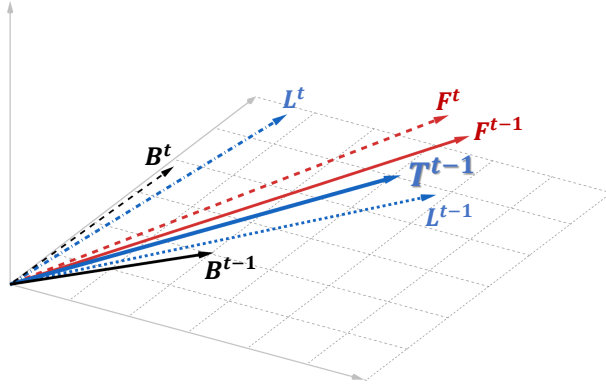


Figure 3: An illustration of TBS. Since the feature space is high-dimensional, we illustrate it using schematic diagrams.

is relatively small, facilitating the combination of L^{t-1} and L^t . Finally, we obtain the binarized DM’s output with TBS applied as $T^{t-1} = (1 - \alpha) \cdot L^{t-1} + \alpha \cdot L^t$, closest to the output F^{t-1} of the full-precision model. The learnable tiny convolution k in TBS allows scaling factors to adapt more flexibly to the representation of DM, while connections across timesteps enable the binarized DM to use the previous step’s output information for appropriate information compensation.

3.3 Space Patched Distillation

Due to the nature of generative models, the optimization process of diffusion models exhibits different characteristics from past discriminative models:

Observation 2. *Conventional distillation struggles to guide fully binarized DMs to align with full-precision DMs, while the features of DM exhibit locality in space during the generation task.*

In previous practices, adding distillation loss during the training of quantized models has been a common approach. As the numerical space of binary models is limited, directly optimizing them using naive loss leads to difficulties in adjusting gradient update directions and makes learning challenging. Therefore, adding distillation loss to intermediate features can better guide the model’s local and global optimization process.

However, as a generative model, the highly rich feature representation of DMs makes it extremely difficult for binary models to finely mimic full-precision models. Although the L2 loss used in the original DM training aligns with the Gaussian noise in the diffusion process, it is not suitable for the distillation matching of intermediate features. During regular distillation, the commonly used L2 loss tends to prioritize optimizing pixels with larger discrepancies, leading to a more uniform and smooth optimization result. This global constraint learning process is challenging for binary models aimed at image generation, as their limited representation capacity makes it difficult for fine-grained distillation imitation to directly adjust them to fully match the direction of full-precision models.

At the same time, we note that DMs using U-Net as a backbone naturally exhibit spatial locality due to their convolution-based structure and generative task requirements. This is different from past discriminative models, where tasks like classification only require overall feature extraction without low-level requirements, making traditional distillation methods unsuitable for DMs with spatial locality in generative tasks. Additionally, most existing DM distillation methods focus on reducing the number of timesteps and do not address the spatial locality of features required for image generation tasks.

Therefore, given the difficulty in optimizing binary DMs with existing loss functions and the spatial locality of DMs, we propose Space Patched Distillation (SPD). Specifically, we designed a new loss function that partitions features into patches before distillation and then calculates spatial attention-guided loss patch by patch. While conventional L2 loss makes it difficult for binary DMs to achieve direct matching, leading to optimization challenges, the attention mechanism allows the distillation

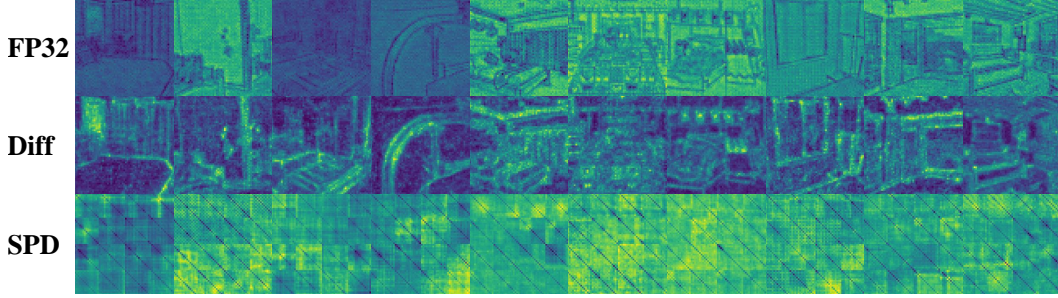


Figure 4: Visualization of the last TimeStepBlock’s output of the LDM model on LSUN-bedroom dataset. FP32 denotes the full-precision model’s output \mathcal{F}^{fp} . Diff denotes the difference between the output of the full-precision model and the binarized one $\|\mathcal{F}^{\text{fp}} - \mathcal{F}^{\text{bi}}\|$. Ours denotes the attention-guided SPD.

optimization to focus more on critical parts. However, this is still challenging for fully binarized DMs because the highly discrete binary outputs have limited information, making it difficult for the model to capture global information. Therefore, we leverage the spatial locality of DMs by dividing intermediate features into multiple patches and independently calculating spatial attention-guided loss for each patch, allowing the binary model to better utilize local information during optimization.

SPD first divides the intermediate features \mathcal{F}^{bi} and $\mathcal{F}^{\text{fp}} \in \mathbb{F}^{b \times c \times w \times h}$, output by a block of the binary DM and the full-precision DM respectively, into p^2 patches:

$$\mathcal{P}_{i,j}^{\text{fp}} = \mathcal{F}_{[:, :, i:i+w/p, j:j+h/p]}^{\text{fp}}, \quad \mathcal{P}_{i,j}^{\text{bi}} = \mathcal{F}_{[:, :, i:i+w/p, j:j+h/p]}^{\text{bi}}. \quad (13)$$

Then, attention-guided loss is calculated for each patch separately:

$$\mathcal{A}_{i,j}^{\text{fp}} = \mathcal{P}_{i,j}^{\text{fp}} \mathcal{P}_{i,j}^{\text{fp}T}, \quad \mathcal{A}_{i,j}^{\text{bi}} = \mathcal{P}_{i,j}^{\text{bi}} \mathcal{P}_{i,j}^{\text{bi}T}. \quad (14)$$

After regularization, the losses at corresponding positions are calculated and summed up:

$$\mathcal{L}_{\text{SPD}}^m = \frac{1}{p^2} \sum_{i=0}^{p-1} \sum_{j=0}^{p-1} \left\| \frac{\mathcal{A}_{i,j}^{\text{fp}}}{\|\mathcal{A}_{i,j}^{\text{fp}}\|_2} - \frac{\mathcal{A}_{i,j}^{\text{bi}}}{\|\mathcal{A}_{i,j}^{\text{bi}}\|_2} \right\|_2, \quad (15)$$

where $\|\cdot\|_2$ denotes the L2 function. Finally, the total training loss \mathcal{L} is computed as:

$$\mathcal{L} = \mathcal{L}_{\text{DM}} + \frac{\lambda}{2d+1} \sum_m^{2d+1} \mathcal{L}_{\text{SPD}}^m, \quad (16)$$

where d denotes the number of blocks during the upsampling process or downsampling process, resulting in a total of $2d + 1$ intermediate features, including the middle block. λ is a hyperparameter coefficient to balance the loss terms, defaulting set to 4.

We visualize the intermediate features and attention-guided SPD mentioned above. As Figure 4 shown, our SPD allows the model to pay more attention to local information in each patch.

4 Experiment

We conduct experiments on various datasets, including CIFAR-10 32×32 [27], LSUN-Bedrooms 256×256 [72], LSUN-Churches 256×256 [72] and FFHQ 256×256 [25] over pixel space diffusion models [19] and latent space diffusion models [50]. The evaluation metrics used in our study encompass Inception Score (IS), Fréchet Inception Distance (FID) [17], Sliding Fréchet Inception Distance (sFID) [52], Precision and Recall. To date, there has been no research that compresses diffusion models to such an extreme extent. Therefore, we use classical binarization algorithms [2; 78; 33; 49], the recent SOTA general binarization algorithms [62], and quantization methods suited to generative models [15; 63] as baselines. We extract the outputs of TimestepEmbedBlocks from the DM to serve as the operating target for our TBS and SPD. And we employ the same shortcut connections in convolutional layers as those used in ReActNet[33]. Detailed experiment settings are presented in the Appendix A.

4.1 Main Results

Pixel Space Diffusion Models. We first conduct experiments on the CIFAR-10 32×32 dataset. As the results presented in Table 1, W1A1 binarization of DM using baseline methods results in substantial degradation. However, BiDM demonstrated significant improvements across all metrics, achieving unprecedented restoration of image quality. Specifically, BiDM achieved remarkable enhancements from 4.23 to 5.18 in the IS metric, and reduced 27.9% in the FID metric.

Table 1: Binarization results for DDIM on CIFAR-10 datasets with 100 steps.

Model	Dataset	Method	#Bits	IS \uparrow	FID \downarrow	sFID \downarrow	Precision \uparrow
DDIM	CIFAR-10 32×32	FP	32/32	8.90	5.54	4.46	67.92
		XNOR++[2]	1/1	2.23	251.14	60.85	44.98
		DoReFa[78]	1/1	1.43	397.60	139.97	0.17
		ReActNet[33]	1/1	3.35	231.55	119.80	18.37
		ReSTE[62]	1/1	1.26	394.29	125.84	0.18
		XNOR[49]	1/1	4.23	113.36	27.67	46.96
		BiDM	1/1	5.18	81.65	25.68	52.92

Latent Space Diffusion Models. Our LDM experiments encompass the evaluation of LDM-4 on LSUN-Bedrooms 256×256 and FFHQ 256×256 datasets, along with the assessment of LDM-8 on the LSUN-Churches 256×256 dataset. The experiments utilized the DDIM sampler with 200 steps, and the detailed outcomes are presented in Table 2. Across these three datasets, our method achieved significant improvements over the best baseline methods. In comparison to other binarization algorithms, BiDM outperformed across all metrics. On the LSUN-Bedrooms, LSUN-Churches, and FFHQ datasets, the FID metric of BiDM decreased by 61.7%, 30.7%, and 51.4%, respectively, compared to the best results among the baselines.

In contrast to XNOR++, its adoption of fixed activation scaling factors in the denoising process results in a very limited dynamic range for its activations, making it difficult to match the highly flexible generative representations of DMs. BiDM addressed this challenge by making the tiny convolution k learnable, which acts on the dynamically computed scaling factors. This optimization led to substantial improvements exceeding an order of magnitude across all metrics. On the LSUN-Bedrooms and LSUN-Churches datasets, the FID metric decreased from 319.66 to 22.74 and from 292.48 to 29.70, respectively. Additionally, compared to the SOTA binarization method ReSTE, BiDM achieved significant enhancements across multiple metrics, particularly demonstrating notable improvements on the LSUN-Bedrooms dataset. We have supplemented our work with BBCU, a binarization method more akin to generative models like DMs rather than discriminative models. Experimental results indicate that even as a binarization strategy for generative models, BBCU faces significant breakdowns when applied to DMs, as FID dropped dramatically to 236.07 on LSUN-Bedrooms. As a work targeting QAT for DM, EfficientDM is indeed a suitable comparison, especially since it designs TALSQ to address the variation in activation range. The results show that EfficientDM struggles to adapt to the extreme scenario of W1A1, and this may be due to its quantizer having difficulty adapting to binarized DM, and using QALoRA for weight updates might yield suboptimal results compared to full-parameter QAT.

As we mentioned in the TBS section of our manuscript, most existing binarization methods struggle to handle the wide activation range and flexible expression of DMs, further highlighting the necessity of TBS. Their optimization strategies may also not be tailored for the image generation tasks performed by DM, which means they only achieve conventional but suboptimal optimization.

4.2 Ablation Study

We perform comprehensive ablation studies for LDM-4 on the LSUN-Bedrooms 256×256 dataset to evaluate the effectiveness of each proposed component in BiDM. We evaluate the effectiveness of our proposed SPD and TBS, and the results are presented in Table 3. Upon separately applying our SPD or TBS methods to LDM, we observed significant improvements compared to the original performance. When the TBS method was incorporated, FID and sFID dropped sharply from 106.62 and 56.61 to 35.23 and 25.13, respectively. Similarly, when the SPD method was added, FID and sFID decreased

Table 2: Quantization results for LDM on LSUN-Bedrooms, LSUN-Churches and FFHQ datasets.

Model	Dataset	Method	#Bits	FID↓	sFID↓	Precision↑	Recall↑
LDM-4	LSUN-Bedrooms 256 × 256	FP	32/32	2.99	7.08	65.02	47.54
		XNOR++	1/1	319.66	184.75	0.00	0.00
		BBCU	1/1	236.07	89.66	0.59	5.66
		EfficientDM	1/1	194.45	113.24	0.99	9.20
		DoReFa	1/1	188.30	89.28	0.86	0.18
		ReActNet	1/1	154.74	61.50	4.63	9.30
		ReSTE	1/1	59.44	42.16	12.06	2.92
		BiDM	1/1	22.74	17.91	33.54	19.90
LDM-8	LSUN-Churches 256 × 256	FP	32/32	4.36	16.00	74.64	48.98
		XNOR++	1/1	292.48	168.65	0.02	0.00
		DoReFa	1/1	162.06	95.37	7.85	0.74
		ReActNet	1/1	56.39	54.68	45.13	2.06
		ReSTE	1/1	47.88	52.44	51.98	3.34
		XNOR	1/1	42.87	49.24	51.53	4.28
		BiDM	1/1	29.70	45.14	55.75	14.80
LDM-4	FFHQ 256 × 256	FP	32/32	4.87	6.96	74.73	50.57
		XNOR++	1/1	379.49	320.64	0.00	0.00
		DoReFa	1/1	214.06	177.63	2.09	0.00
		ReActNet	1/1	147.88	141.31	3.36	0.69
		ReSTE	1/1	144.37	97.43	4.03	0.03
		XNOR	1/1	89.37	54.04	31.31	4.11
		BiDM	1/1	43.42	32.35	49.44	13.96

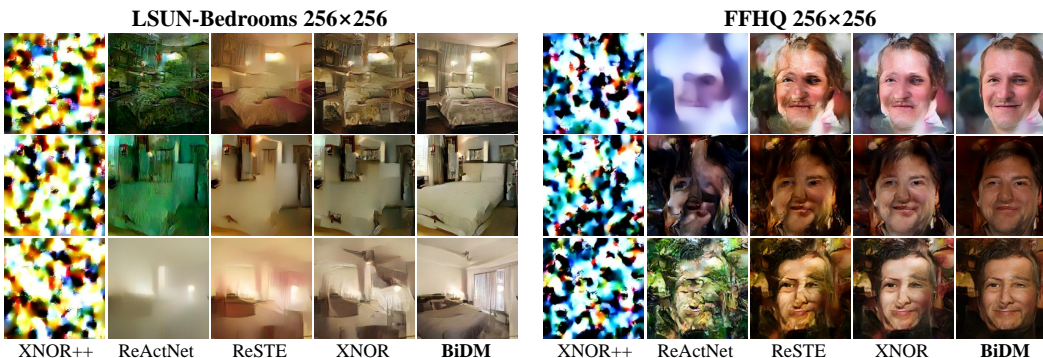


Figure 5: Visualization of samples generated by the W1A1 baseline and our BiDM. BiDM is the first fully binarized DM method capable of generating viewable images, significantly surpassing advanced binarization methods.

significantly from 106.62 and 56.61 to 40.62 and 31.61, respectively. Other metrics also exhibited substantial improvements. This demonstrates the effectiveness of our approach in continuously approximating the binarized model features to full-precision features during training by introducing a learnable factor α_m^t and incorporating connections between adjacent time steps. Furthermore, when we combined our two methods and applied them to LDM, we observed an additional improvement compared to the individual application of each method. This further substantiates that performing distillation between full-precision and binarized models at the patch level can significantly enhance the performance of the binarized model. We also conducted additional ablation experiments, and the results are presented in the appendix B.

Table 3: Ablation result of each proposed component.

Method	#Bits	FID↓	sFID↓	Prec.↑	Recall↑
Vanilla	1/1	106.62	56.81	6.82	5.22
+TBS	1/1	35.23	25.13	26.38	14.32
+SPD	1/1	40.62	31.61	23.87	11.18
BiDM	1/1	22.74	17.91	33.54	19.90

4.3 Efficiency Analysis

Inference Efficiency Analysis. We conducted an analysis of the diffusion model’s inference efficiency under complete binarization. During inference, BiDM requires only a very small number of additional floating-point additions for the connections across timesteps compared to the classic binarization work XNOR-Net, and there are no differences in the majority of calculations, such as convolutions. Performing a floating-point convolution with a depth of 1 for scaling factors requires only a small amount of computation, and the overhead for averaging matrix A is also minimal. The findings presented in Table 4 reveal that BiDM, while achieving the same $28.0\times$ memory efficiency and $52.7\times$ computational savings as the XNOR baseline, demonstrates significantly superior image generation capabilities, with the FID decreased from 106.62 to 22.74. See Appendix B for more details.

Table 4: Inference efficiency of our proposed BiDM of LDM-4 on LSUN-Bedrooms.

Method	#Bits	Size(MB)	BOPs($\times 10^9$)	FLOPs($\times 10^9$)	OPs($\times 10^9$)	FID↓
FP	32/32	1045.4	-	96.00	96.00	2.99
XNOR	1/1	37.3	92.1	0.38	1.82	106.62
BiDM	1/1	37.3	92.1	0.38	1.82	22.74

Training Efficiency Analysis. We also explored the training efficiency of BiDM, as the overhead required for the QAT of binarized DMs cannot be overlooked. Theoretical analysis and experimental results show that BiDM achieved significantly better generative results than baseline methods under the same training cost, demonstrating that it not only has a higher upper limit of generative capability but is also relatively efficient in terms of generative performance. See Appendix B for details.

Limitations. The techniques of BiDM increase the training time of DMs compared with the original process, and future efforts may thus focus on the efficient quantization process of DMs.

5 Conclusion.

In this paper, we present BiDM, a novel fully binarized method that pushes the compression of diffusion models to the limit. Based on two observations — activations at different timesteps and the characteristics of image generation tasks — we propose the Timestep-friendly Binary Structure (TBS) and Space Patched Distillation (SPD) from temporal and spatial perspectives, respectively. These methods address the severe limitations in representation capacity and the challenges of highly discrete spatial optimization in full binarization. As the first fully binarized diffusion model, BiDM demonstrates significantly better generative performance than the SOTA general binarization methods across multiple models and datasets. On LSUN-Bedrooms, BiDM achieves an FID of 22.74, greatly surpassing the SOTA method with an FID of 59.44, making it the only method capable of generating visually acceptable samples while achieving up to $28.0\times$ storage savings and $52.7\times$ OPs savings.

Acknowledgments and Disclosure of Funding

This work was supported by the Beijing Municipal Science and Technology Project (No. Z231100010323002), the National Natural Science Foundation of China (Nos. 62306025, 92367204), and the Fundamental Research Funds for the Central Universities.

References

- [1] Thomas Bird, Friso H Kingma, and David Barber. Reducing the computational cost of deep generative models with binary neural networks. *arXiv preprint arXiv:2010.13476*, 2020.
- [2] Adrian Bulat and Georgios Tzimiropoulos. Xnor-net++: Improved binary neural networks. *arXiv preprint arXiv:1909.13863*, pages 1–12, 2019.
- [3] Zhaowei Cai and Nuno Vasconcelos. Rethinking differentiable search for mixed-precision neural networks. In *Proceedings of the IEEE/CVF Conference on Computer Vision and Pattern Recognition*, pages 2349–2358, 2020.
- [4] Zheng Chen, Haotong Qin, Yong Guo, Xiongfei Su, Xin Yuan, Linghe Kong, and Yulun Zhang. Binarized diffusion model for image super-resolution. *arXiv preprint arXiv:2406.05723*, 2024.
- [5] Matthieu Courbariaux, Itay Hubara, Daniel Soudry, Ran El-Yaniv, and Yoshua Bengio. Binarized neural networks: Training deep neural networks with weights and activations constrained to+ 1 or-1. *arXiv preprint arXiv:1602.02830*, pages 1–11, 2016.
- [6] Steven K Esser, Jeffrey L McKinstry, Deepika Bablani, Rathinakumar Appuswamy, and Dharmendra S Modha. Learned step size quantization. In *International Conference on Learning Representations*, pages 1–12, 2019.
- [7] Gongfan Fang, Xinyin Ma, and Xinchao Wang. Structural pruning for diffusion models. *arXiv preprint arXiv:2305.10924*, 2023.
- [8] Lukas Geiger and Plumerai Team. Larq: An open-source library for training binarized neural networks. *Journal of Open Source Software*, 5(45):1746, 2020.
- [9] Amir Gholami, Sehoon Kim, Zhen Dong, Zhewei Yao, Michael W Mahoney, and Kurt Keutzer. A survey of quantization methods for efficient neural network inference. In *Low-Power Computer Vision*, pages 291–326. Chapman and Hall/CRC, 2022.
- [10] Ruihao Gong, Yifu Ding, Zining Wang, Chengtao Lv, Xingyu Zheng, Jinyang Du, Haotong Qin, Jinyang Guo, Michele Magno, and Xianglong Liu. A survey of low-bit large language models: Basics, systems, and algorithms. *arXiv preprint arXiv:2409.16694*, 2024.
- [11] Guangyu Guo, Longfei Han, Le Wang, Dingwen Zhang, and Junwei Han. Semantic-aware knowledge distillation with parameter-free feature uniformization. *Visual Intelligence*, 1(1):6, 2023.
- [12] Jinyang Guo, Jiaheng Liu, and Dong Xu. Jointpruning: Pruning networks along multiple dimensions for efficient point cloud processing. *IEEE Transactions on Circuits and Systems for Video Technology*, 32(6):3659–3672, 2021.
- [13] Jinyang Guo, Jiaheng Liu, and Dong Xu. 3d-pruning: A model compression framework for efficient 3d action recognition. *IEEE Transactions on Circuits and Systems for Video Technology*, 32(12):8717–8729, 2022.
- [14] Jinyang Guo, Dong Xu, and Wanli Ouyang. Multidimensional pruning and its extension: A unified framework for model compression. *IEEE Transactions on Neural Networks and Learning Systems*, 2023.
- [15] Yefei He, Jing Liu, Weijia Wu, Hong Zhou, and Bohan Zhuang. Efficientdm: Efficient quantization-aware fine-tuning of low-bit diffusion models. *arXiv preprint arXiv:2310.03270*, 2023.
- [16] Yefei He, Zhenyu Lou, Luoming Zhang, Jing Liu, Weijia Wu, Hong Zhou, and Bohan Zhuang. Bivit: Extremely compressed binary vision transformers. In *Proceedings of the IEEE/CVF International Conference on Computer Vision*, pages 5651–5663, 2023.
- [17] Martin Heusel, Hubert Ramsauer, Thomas Unterthiner, Bernhard Nessler, and Sepp Hochreiter. Gans trained by a two time-scale update rule converge to a local nash equilibrium. *Advances in neural information processing systems*, 30, 2017.

- [18] Jonathan Ho, William Chan, Chitwan Saharia, Jay Whang, Ruiqi Gao, Alexey Gritsenko, Diederik P Kingma, Ben Poole, Mohammad Norouzi, David J Fleet, et al. Imagen video: High definition video generation with diffusion models. *arXiv preprint arXiv:2210.02303*, 2022.
- [19] Jonathan Ho, Ajay Jain, and Pieter Abbeel. Denoising diffusion probabilistic models. *Advances in neural information processing systems*, 33:6840–6851, 2020.
- [20] Wei Huang, Yangdong Liu, Haotong Qin, Ying Li, Shiming Zhang, Xianglong Liu, Michele Magno, and Xiaojuan Qi. Billm: Pushing the limit of post-training quantization for llms. *arXiv preprint arXiv:2402.04291*, 2024.
- [21] Wei Huang, Xudong Ma, Haotong Qin, Xingyu Zheng, Chengtao Lv, Hong Chen, Jie Luo, Xiaojuan Qi, Xianglong Liu, and Michele Magno. How good are low-bit quantized llama3 models? an empirical study. *arXiv preprint arXiv:2404.14047*, 2024.
- [22] Yushi Huang, Ruihao Gong, Jing Liu, Tianlong Chen, and Xianglong Liu. Tfmq-dm: Temporal feature maintenance quantization for diffusion models. *arXiv preprint arXiv:2311.16503*, 2023.
- [23] Itay Hubara, Matthieu Courbariaux, Daniel Soudry, Ran El-Yaniv, and Yoshua Bengio. Binarized neural networks. *Advances in Neural Information Processing Systems*, 29:1–9, 2016.
- [24] Myeonghun Jeong, Hyeongju Kim, Sung Jun Cheon, Byoung Jin Choi, and Nam Soo Kim. Diff-tts: A denoising diffusion model for text-to-speech. *arXiv preprint arXiv:2104.01409*, 2021.
- [25] Tero Karras, Samuli Laine, and Timo Aila. A style-based generator architecture for generative adversarial networks. In *Proceedings of the IEEE/CVF conference on computer vision and pattern recognition*, pages 4401–4410, 2019.
- [26] Diederik P Kingma and Max Welling. Auto-encoding variational bayes. *arXiv preprint arXiv:1312.6114*, 2013.
- [27] Alex Krizhevsky, Geoffrey Hinton, et al. Learning multiple layers of features from tiny images. pages 1–60, 2009.
- [28] Phuoc-Hoan Charles Le and Xinlin Li. Binaryvit: pushing binary vision transformers towards convolutional models. In *Proceedings of the IEEE/CVF Conference on Computer Vision and Pattern Recognition*, pages 4664–4673, 2023.
- [29] Xiuyu Li, Yijiang Liu, Long Lian, Huanrui Yang, Zhen Dong, Daniel Kang, Shanghang Zhang, and Kurt Keutzer. Q-diffusion: Quantizing diffusion models. In *Proceedings of the IEEE/CVF International Conference on Computer Vision*, pages 17535–17545, 2023.
- [30] Yanjing Li, Sheng Xu, Xianbin Cao, Xiao Sun, and Baochang Zhang. Q-dm: An efficient low-bit quantized diffusion model. In *Thirty-seventh Conference on Neural Information Processing Systems*, 2023.
- [31] Luping Liu, Yi Ren, Zhijie Lin, and Zhou Zhao. Pseudo numerical methods for diffusion models on manifolds. *arXiv preprint arXiv:2202.09778*, 2022.
- [32] Zechun Liu, Wenhan Luo, Baoyuan Wu, Xin Yang, Wei Liu, and Kwang-Ting Cheng. Bi-real net: Binarizing deep network towards real-network performance. *International Journal of Computer Vision*, 128:202–219, 2020.
- [33] Zechun Liu, Zhiqiang Shen, Marios Savvides, and Kwang-Ting Cheng. Reactnet: Towards precise binary neural network with generalized activation functions. In *Proceedings of the European Conference on Computer Vision*, pages 143–159. Springer, 2020.
- [34] Cheng Lu, Yuhao Zhou, Fan Bao, Jianfei Chen, Chongxuan Li, and Jun Zhu. Dpm-solver: A fast ode solver for diffusion probabilistic model sampling in around 10 steps. *Advances in Neural Information Processing Systems*, 35:5775–5787, 2022.
- [35] Cheng Lu, Yuhao Zhou, Fan Bao, Jianfei Chen, Chongxuan Li, and Jun Zhu. Dpm-solver++: Fast solver for guided sampling of diffusion probabilistic models. *arXiv preprint arXiv:2211.01095*, 2022.

- [36] Weijian Luo. A comprehensive survey on knowledge distillation of diffusion models. *arXiv preprint arXiv:2304.04262*, 2023.
- [37] Chengtao Lv, Hong Chen, Jinyang Guo, Yifu Ding, and Xianglong Liu. Ptq4sam: Post-training quantization for segment anything. In *Proceedings of the IEEE/CVF Conference on Computer Vision and Pattern Recognition*, pages 15941–15951, 2024.
- [38] Xinyin Ma, Gongfan Fang, and Xinchao Wang. Deepcache: Accelerating diffusion models for free. *arXiv preprint arXiv:2312.00858*, 2023.
- [39] Brais Martinez, Jing Yang, Adrian Bulat, and Georgios Tzimiropoulos. Training binary neural networks with real-to-binary convolutions. *arXiv preprint arXiv:2003.11535*, 2020.
- [40] Kangfu Mei and Vishal Patel. Vidm: Video implicit diffusion models. In *Proceedings of the AAAI Conference on Artificial Intelligence*, volume 37, pages 9117–9125, 2023.
- [41] Chenlin Meng, Robin Rombach, Ruiqi Gao, Diederik Kingma, Stefano Ermon, Jonathan Ho, and Tim Salimans. On distillation of guided diffusion models. In *Proceedings of the IEEE/CVF Conference on Computer Vision and Pattern Recognition*, pages 14297–14306, 2023.
- [42] Gautam Mittal, Jesse Engel, Curtis Hawthorne, and Ian Simon. Symbolic music generation with diffusion models. *arXiv preprint arXiv:2103.16091*, 2021.
- [43] Chenhao Niu, Yang Song, Jiaming Song, Shengjia Zhao, Aditya Grover, and Stefano Ermon. Permutation invariant graph generation via score-based generative modeling. In *International Conference on Artificial Intelligence and Statistics*, pages 4474–4484. PMLR, 2020.
- [44] William Peebles and Saining Xie. Scalable diffusion models with transformers. In *Proceedings of the IEEE/CVF International Conference on Computer Vision*, pages 4195–4205, 2023.
- [45] Vadim Popov, Ivan Vovk, Vladimir Gogoryan, Tasnima Sadekova, and Mikhail Kudinov. Grad-tts: A diffusion probabilistic model for text-to-speech. In *International Conference on Machine Learning*, pages 8599–8608. PMLR, 2021.
- [46] Haotong Qin, Ruihao Gong, Xianglong Liu, Mingzhu Shen, Ziran Wei, Fengwei Yu, and Jingkuan Song. Forward and backward information retention for accurate binary neural networks. In *Proceedings of the IEEE/CVF Conference on Computer Vision and Pattern Recognition*, pages 2250–2259, 2020.
- [47] Haotong Qin, Xudong Ma, Xingyu Zheng, Xiaoyang Li, Yang Zhang, Shouda Liu, Jie Luo, Xianglong Liu, and Michele Magno. Accurate lora-finetuning quantization of llms via information retention. *arXiv preprint arXiv:2402.05445*, 2024.
- [48] Haotong Qin, Xiangguo Zhang, Ruihao Gong, Yifu Ding, Yi Xu, and Xianglong Liu. Distribution-sensitive information retention for accurate binary neural network. *International Journal of Computer Vision*, 131(1):26–47, 2023.
- [49] Mohammad Rastegari, Vicente Ordonez, Joseph Redmon, and Ali Farhadi. Xnor-net: Imagenet classification using binary convolutional neural networks. In *Proceedings of the European Conference on Computer Vision*, pages 525–542. Springer, 2016.
- [50] Robin Rombach, Andreas Blattmann, Dominik Lorenz, Patrick Esser, and Björn Ommer. High-resolution image synthesis with latent diffusion models, 2021.
- [51] Olaf Ronneberger, Philipp Fischer, and Thomas Brox. U-net: Convolutional networks for biomedical image segmentation. In *Medical image computing and computer-assisted intervention—MICCAI 2015: 18th international conference, Munich, Germany, October 5-9, 2015, proceedings, part III 18*, pages 234–241. Springer, 2015.
- [52] Tim Salimans, Ian Goodfellow, Wojciech Zaremba, Vicki Cheung, Alec Radford, and Xi Chen. Improved techniques for training gans. *Advances in neural information processing systems*, 29, 2016.
- [53] Tim Salimans and Jonathan Ho. Progressive distillation for fast sampling of diffusion models. *arXiv preprint arXiv:2202.00512*, 2022.

- [54] Yuzhang Shang, Zhihang Yuan, Bin Xie, Bingzhe Wu, and Yan Yan. Post-training quantization on diffusion models. In *Proceedings of the IEEE/CVF Conference on Computer Vision and Pattern Recognition*, pages 1972–1981, 2023.
- [55] Junhyuk So, Jungwon Lee, Daehyun Ahn, Hyungjun Kim, and Eunhyeok Park. Temporal dynamic quantization for diffusion models. *Advances in Neural Information Processing Systems*, 36, 2024.
- [56] Jiaming Song, Chenlin Meng, and Stefano Ermon. Denoising diffusion implicit models. *arXiv preprint arXiv:2010.02502*, 2020.
- [57] Yang Song and Stefano Ermon. Generative modeling by estimating gradients of the data distribution. *Advances in neural information processing systems*, 32, 2019.
- [58] Yang Song, Jascha Sohl-Dickstein, Diederik P Kingma, Abhishek Kumar, Stefano Ermon, and Ben Poole. Score-based generative modeling through stochastic differential equations. *arXiv preprint arXiv:2011.13456*, 2020.
- [59] Jia-Mu Sun, Tong Wu, and Lin Gao. Recent advances in implicit representation-based 3d shape generation. *Visual Intelligence*, 2(1):9, 2024.
- [60] Peisong Wang, Xiangyu He, Gang Li, Tianli Zhao, and Jian Cheng. Sparsity-inducing binarized neural networks. In *Proceedings of the AAAI Conference on Artificial Intelligence*, volume 34, pages 12192–12199, 2020.
- [61] Ze Wang, Jiang Wang, Zicheng Liu, and Qiang Qiu. Binary latent diffusion. In *Proceedings of the IEEE/CVF Conference on Computer Vision and Pattern Recognition*, pages 22576–22585, 2023.
- [62] Xiao-Ming Wu, Dian Zheng, Zuhao Liu, and Wei-Shi Zheng. Estimator meets equilibrium perspective: A rectified straight through estimator for binary neural networks training. In *Proceedings of the IEEE/CVF International Conference on Computer Vision*, pages 17055–17064, 2023.
- [63] Bin Xia, Yulun Zhang, Yitong Wang, Yapeng Tian, Wenming Yang, Radu Timofte, and Luc Van Gool. Basic binary convolution unit for binarized image restoration network. *arXiv preprint arXiv:2210.00405*, 2022.
- [64] Yisong Xiao, Aishan Liu, Tianyuan Zhang, Haotong Qin, Jinyang Guo, and Xianglong Liu. Robustmq: benchmarking robustness of quantized models. *Visual Intelligence*, 1(1):30, 2023.
- [65] Yixing Xu, Kai Han, Chang Xu, Yehui Tang, Chunjing Xu, and Yunhe Wang. Learning frequency domain approximation for binary neural networks. *Advances in Neural Information Processing Systems*, 34:25553–25565, 2021.
- [66] Zhekai Xu, Haohong Shang, Shaoze Yang, Ruiqi Xu, Yichao Yan, Yixuan Li, Jiawei Huang, Howard C Yang, and Jianjun Zhou. Hierarchical painter: Chinese landscape painting restoration with fine-grained styles. *Visual Intelligence*, 1(1):19, 2023.
- [67] Zihan Xu, Mingbao Lin, Jianzhuang Liu, Jie Chen, Ling Shao, Yue Gao, Yonghong Tian, and Rongrong Ji. Recu: Reviving the dead weights in binary neural networks. In *Proceedings of the IEEE/CVF International Conference on Computer Vision*, pages 5198–5208, 2021.
- [68] Yichao Yan, Zanwei Zhou, Zi Wang, Jingnan Gao, and Xiaokang Yang. Dialoguenerf: Towards realistic avatar face-to-face conversation video generation. *Visual Intelligence*, 2(1):24, 2024.
- [69] Jiaming Yang, Chenwei Tang, Caiyang Yu, and Jiancheng Lv. Gwq: Group-wise quantization framework for neural networks. In *Asian Conference on Machine Learning*, pages 1526–1541. PMLR, 2024.
- [70] Jiwei Yang, Xu Shen, Jun Xing, Xinmei Tian, Houqiang Li, Bing Deng, Jianqiang Huang, and Xian-sheng Hua. Quantization networks. In *Proceedings of the IEEE/CVF Conference on Computer Vision and Pattern Recognition*, pages 7308–7316, 2019.

- [71] Kai-Lang Yao and Wu-Jun Li. Full-precision free binary graph neural networks. 2021.
- [72] Fisher Yu, Ari Seff, Yinda Zhang, Shuran Song, Thomas Funkhouser, and Jianxiong Xiao. Lsun: Construction of a large-scale image dataset using deep learning with humans in the loop. *arXiv preprint arXiv:1506.03365*, 2015.
- [73] Zelong Zeng, Fan Yang, Hong Liu, and Shin’ichi Satoh. Improving deep metric learning via self-distillation and online batch diffusion process. *Visual Intelligence*, 2(1):18, 2024.
- [74] Jianhao Zhang, Yingwei Pan, Ting Yao, He Zhao, and Tao Mei. Dabnn: A super fast inference framework for binary neural networks on arm devices. In *Proceedings of the 27th ACM International Conference on Multimedia*, pages 2272–2275, 2019.
- [75] Yulun Zhang, Haotong Qin, Zixiang Zhao, Xianglong Liu, Martin Danelljan, and Fisher Yu. Flexible residual binarization for image super-resolution. In Ruslan Salakhutdinov, Zico Kolter, Katherine Heller, Adrian Weller, Nuria Oliver, Jonathan Scarlett, and Felix Berkenkamp, editors, *Proceedings of the 41st International Conference on Machine Learning*, volume 235 of *Proceedings of Machine Learning Research*, pages 59731–59740. PMLR, 21–27 Jul 2024.
- [76] Wenliang Zhao, Haolin Wang, Jie Zhou, and Jiwen Lu. Dc-solver: Improving predictor-corrector diffusion sampler via dynamic compensation. *arXiv preprint arXiv:2409.03755*, 2024.
- [77] Xingyu Zheng, Haotong Qin, Xudong Ma, Mingyuan Zhang, Haojie Hao, Jiakai Wang, Zixiang Zhao, Jinyang Guo, and Xianglong Liu. Binarydm: Towards accurate binarization of diffusion model. *arXiv preprint arXiv:2404.05662*, 2024.
- [78] Shuchang Zhou, Yuxin Wu, Zekun Ni, Xinyu Zhou, He Wen, and Yuheng Zou. Dorefa-net: Training low bitwidth convolutional neural networks with low bitwidth gradients. *arXiv preprint arXiv:1606.06160*, pages 1–13, 2016.

A Experiment Settings

We adopt several classic binarization algorithms, including XNOR [49], XNOR++ [2], DoReFa [78], and ReActNet [33], along with the SOTA binarization method, ReSTE [62] as baselines. Additionally, we also include the quantization methods designed for generative models, BBCU [63] and EfficientDM [15]. We extract the output features of TimestepEmbedBlocks from the DM to serve as the targets of TBS and SPD operations. For the CIFAR-10 [27] dataset, We add TBS connections to the outputs of the last 2 timestep embedding blocks and set α_{init} to 0.3. The λ on CIFAR-10 is set to $3e-2$. For the LSUN-Bedrooms [72], LSUN-Churches [72] and FFHQ [25] datasets, We add TBS connections to the outputs of the last 8 timestep embedding blocks and also set α_{init} to 0.3. The λ on these three datasets is set to $1e-2$.

Our quantization-aware training is based on the pre-trained diffusion model, and the quantizer parameters and latent weights are trained simultaneously. The overall training process is relatively consistent with the original training process of DDIM or LDM. For the CIFAR-10 dataset, we set the learning rate to $6e-5$ and the batch size to 64 during training. The training process consisted of 100k iterations, and during sampling, we used 100 sampling steps. For the LSUN-Bedrooms, LSUN-Churches and FFHQ datasets, the learning rate was set to $2e-5$ and the batch size to 4 during training. The training consisted of 200k iterations, with 200 steps used during denoising phase.

We conducted extensive experiments on two different types of diffusion models: the latent-space diffusion model LDM and the pixel-space diffusion model DDIM. For the DDIM model, we specifically selected the CIFAR-10 dataset with a resolution of 32×32 for our experiments. For the LDM model, our experiments spanned multiple datasets, including the LSUN-Bedrooms, LSUN-Churches and the FFHQ dataset, all with a resolution of 256×256 . To evaluate the generation quality of the diffusion model, we utilize several evaluation metrics, including Inception Score (IS), Fréchet Inception Distance (FID) [17], Sliding Fréchet Inception Distance (sFID) [52], and Precision-and-Recall. After 200,000 iterations of training, we randomly sample and generate 50,000 images from the model and compute the metrics based on reference batches. The reference batches used to evaluate FID and sFID contain all the corresponding datasets. We recorded FID, sFID, and Precision for all tasks and additional IS for CIFAR-10.

We utilize OPs as metrics for evaluating theoretical inference efficiency. Taking the convolutional unit as an example, the BOPs for a single computation operation of a single convolution are defined as follows $nmk^2b_ab_w$ [69; 71]. It is composed of b_w bits for weights, b_a bits for activation, n input channels, m output channels, and a $k \times k$ convolutional kernel. For the output feature with width w and height h , $BOPs \approx whnmk^2b_ab_w$. As there might also be full-precision modules in the model, the total OPs of the model are summed up as $\frac{1}{64}BOPs + FLOPs$ [3]. All our experiments are conducted on a server with NVIDIA A100 40GB GPU.

B Additional Quantitative Results

We conducted more detailed ablation experiments to comprehensively validate our results.

Effects of learnable k in TBS. We apply the proposed learnable k to the XNOR baseline. The experimental results shown in Table 5 indicate that this modification can lead to a significant improvement in performance. The model achieved a doubling of improvement in FID, sFID. Their original values were 106.62 and 56.81, respectively, and they decreased to 57.62 and 30.46. The negligible degradation in Recall can be overlooked.

Table 5: Solely transforming k into learnable on the XNOR baseline network.

k	#Bits	FID↓	sFID↓	Prec.↑	Recall↑
Vanilla	1/1	106.62	56.81	6.82	5.22
learnable	1/1	57.26	30.46	15.88	5.00

Effects of cross-timestep connection in TBS. We investigated the impact of varying the number of TBS connections. Table 6 illustrates that the introduction of TBS cross-timestep connections consistently outperforms models without such connections ($n = 0$). This validates the efficacy of our cross-timestep linkage strategy based on the high-dimensional feature similarity of LDM. Among

the experiments incorporating cross-timestep connections, the models with 1 and 8 connections both achieved equally optimal results. The model with 1 connection demonstrated slightly superior performance in FID and Precision, whereas the model with 8 nodes exhibited marginally better outcomes in sFID and Recall.

Table 6: The number of TBS connections

n	FID↓	sFID↓	Prec.↑	Recall↑
0	30.24	28.21	29.77	16.94
1	24.22	20.94	34.28	18.22
8	22.74	17.91	33.54	19.90
12	23.25	28.31	37.74	18.78

Effects of SPD. As a general quantization method, real-to-binary [39] suggests that using attention map-based loss during the distillation of a binary model from a full-precision model achieves better results. In contrast, BinaryDM, as the work most closely related to BiDM, directly points out that using L2 loss makes it difficult to align and optimize binary features with full-precision features. These studies indicate that the general L2 loss is inadequate for meeting the optimization needs of binary scenarios. So we also compare our SPD with the commonly used L2 loss function. As shown in Table 7, by replacing the L2 loss function with patch distillation, the model can achieve better performance.

Table 7: Different distillation strategies

\mathcal{L}_{distil}	FID↓	sFID↓	Prec.↑	Recall↑
\mathcal{L}_2	26.07	23.26	33.12	18.98
\mathcal{L}_{SPD}	22.74	17.91	33.54	19.90

Further Inference Efficiency Analysis. We expand upon the inference process described in Eq.9 and provide a detailed explanation and testing. Since the divisor involved in calculating the mean of $A^{1,h,w}$ from $I^{c,h,w}$ (i.e., the channel dimension c) can be integrated into $k^{1,1,3,3}$ in advance, resulting in $k^{1,1,3,3} = \frac{k^{1,1,3,3}}{c}$. Additionally, $\alpha^{n,1,1,1}$ derived from $W^{n,c,h,w}$ can also be computed ahead of inference. Therefore, the actual operations involved during inference are as follows:

[FP] Original full-precision convolution:

- (0) Perform convolution between full-precision $I_f^{c=448,h=32,w=32}$ and full-precision $W_f^{n=448,c=448,h=32,w=32}$ to obtain the full-precision output $O_f^{448,32,32}$.

[XNOR-Net/BiDM] The inference process for XNOR-Net/BiDM involves the following 6 steps:

- Sign operation:
 - (1) Sign operation:
- Binary operation:
 - (2) Perform convolution between the binary $I_b^{448,32,32}$ and the binary $W_b^{448,448,3,3}$ to obtain the full-precision output $O_f^{448,32,32}$.
- Full-precision operations:
 - (3) Sum the full-precision $I_f^{448,32,32}$ across channels to obtain $A^{1,32,32}$.
 - (4) Perform convolution between full-precision $A^{1,32,32}$ and $k^{1,1,3,3}$ to obtain $O_1^{1,32,32}$.
 - (5) Pointwise multiply $O_f^{448,32,32}$ by $O_1^{1,32,32}$ to obtain the full-precision output $O_2^{448,32,32}$.
 - (6) Pointwise multiply $O_2^{448,32,32}$ by $\alpha^{448,1,1}$ to obtain the final full-precision output $O^{448,32,32}$.

We utilized the general deployment library Larq [8] on a Qualcomm Snapdragon 855 Plus to test the actual runtime efficiency of the aforementioned single convolution. The runtime results for a single inference are summarized in the Table 8. Due to limitations of the deployment library and hardware, Baseline achieved a 9.97x speedup, while XNOR-Net / BiDM achieved an 8.07x speedup. Besides, the improvement in generation performance brought by BiDM is even more significant, and we believe that it could achieve better acceleration results in a more optimized environment.

Table 8: The actual runtime efficiency of a single convolution.

Method	(0)	(1)+(2)	(3)	(4)	(5)	(6)	Runtime(μs /convolution)	FID \downarrow
FP	176371.0						176371.0	2.99
Baseline (DoReFa)		17695.2				4.3	17699.5	188.30
XNOR-Net / BiDM		17695.2	2948.8	1133.3	83.2	4.3	21864.8	22.74

Further Training Efficiency Analysis. BiDM consists of two techniques: TBS and SPD. The time efficiency analysis during training is as follows: (1) TBS includes the learnable convolution of scaling factors (Eq.10) and the cross-time step connection (Eq.12). The increase in training time due to the convolution of trainable scaling factors is minimal, as the depth of the convolution for scaling factors is only 1, and the size of the trainable convolution kernel is only 3×3 . The cross-time step connection is the primary factor for the increase in training time. Since it requires training α , we introduce this structure during training, so each training sample requires not only noise estimation for T^{t-1} but also for T^t , directly doubling the sampling steps. (2) SPD may lead to a slight increase in training time (an additional 0.18 times), but since we only apply supervision to the larger upsampling/middle/downsampling blocks, the increase is limited.

The results in Figure 6 align well with the theoretical analysis mentioned above. BiDM achieved significantly better generative results than baseline methods under the same training iterations, demonstrating that it not only has a higher upper limit of generative capability but is also relatively efficient when considering generative performance.

We also tested the FID after uniformly training for 0.5 days, and the results in Tabel 9 show: (1) BiDM has the best convergence, even in a short training time. (2) No.3 significantly outperforms No.5 because connections across timesteps greatly increase training time, making No.3 converge faster in the early training stages. (3) No.5 slightly outperforms No.7 because \mathcal{L}_{SPD} causes a slight increase in training time.

We emphasize that the biggest challenge in fully binarizing DM lies in the drop in accuracy. Although BiDM requires a longer training time for the same number of iters, it significantly enhances the quality of generated images, as no other method has been able to produce effective images.

Table 9: Training speed under different settings, and FID at 0.5 days.

No.	convolution of scaling factors (Eq.9)	learnable k	connections across timesteps	\mathcal{L}_{distil}	Training Speed (ms/iter)	FID \downarrow at 0.5 days
1					309.8	167.59
2	✓				310.2	121.63
3	✓	✓			340.8	58.55
4	✓		✓		458.5	93.66
5	✓	✓	✓		480.2	70.80
6	✓			\mathcal{L}_{SPD}	389.6	86.78
7	✓	✓	✓	\mathcal{L}_2 (MSE)	496.8	71.15
8	✓	✓	✓	\mathcal{L}_{SPD}	547.2	47.11

C Additional Visualization Results

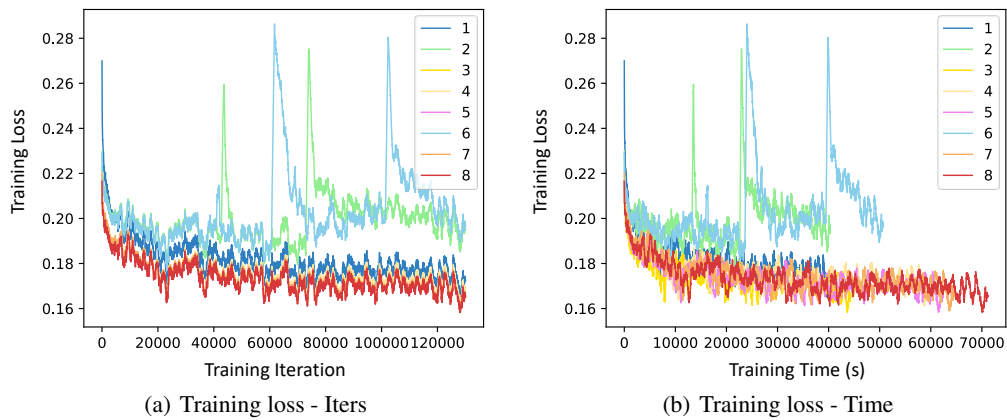


Figure 6: (a) Training iterations and training loss under different settings. (b) Training time and training loss under different settings. The meaning of the numbers in the legend corresponds to those in Table 9.

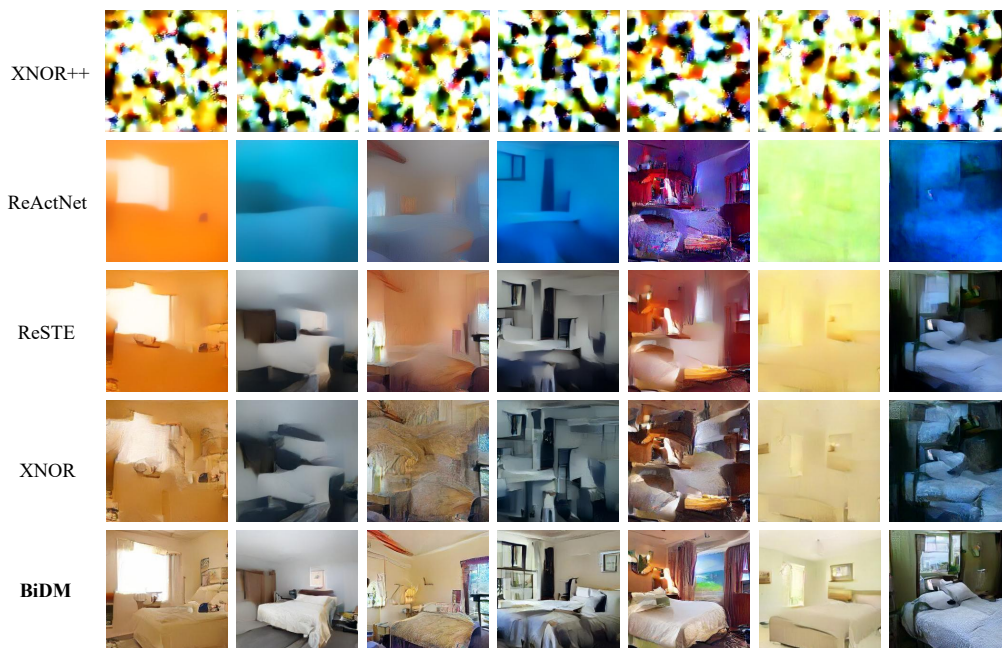


Figure 7: Generation results of BiDM and baselines on the LSUN-Bedrooms dataset.



Figure 8: Generation results of BiDM and baselines on the LSUN-Churches dataset.

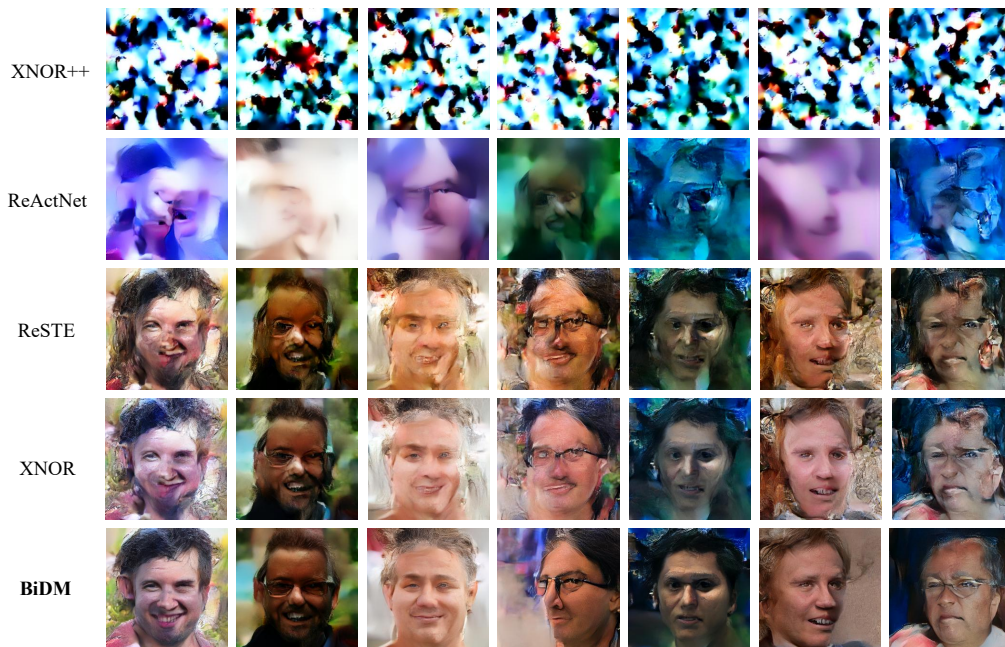


Figure 9: Generation results of BiDM and baselines on the FFHQ dataset.

NeurIPS Paper Checklist

1. Claims

Question: Do the main claims made in the abstract and introduction accurately reflect the paper's contributions and scope?

Answer: [Yes]

Justification: We make the main claims made in the abstract and introduction accurately reflect the paper's contributions and scope.

Guidelines:

- The answer NA means that the abstract and introduction do not include the claims made in the paper.
- The abstract and/or introduction should clearly state the claims made, including the contributions made in the paper and important assumptions and limitations. A No or NA answer to this question will not be perceived well by the reviewers.
- The claims made should match theoretical and experimental results, and reflect how much the results can be expected to generalize to other settings.
- It is fine to include aspirational goals as motivation as long as it is clear that these goals are not attained by the paper.

2. Limitations

Question: Does the paper discuss the limitations of the work performed by the authors?

Answer: [Yes]

Justification: The paper discusses the limitations of the work in section 4.

Guidelines:

- The answer NA means that the paper has no limitation while the answer No means that the paper has limitations, but those are not discussed in the paper.
- The authors are encouraged to create a separate "Limitations" section in their paper.
- The paper should point out any strong assumptions and how robust the results are to violations of these assumptions (e.g., independence assumptions, noiseless settings, model well-specification, asymptotic approximations only holding locally). The authors should reflect on how these assumptions might be violated in practice and what the implications would be.
- The authors should reflect on the scope of the claims made, e.g., if the approach was only tested on a few datasets or with a few runs. In general, empirical results often depend on implicit assumptions, which should be articulated.
- The authors should reflect on the factors that influence the performance of the approach. For example, a facial recognition algorithm may perform poorly when image resolution is low or images are taken in low lighting. Or a speech-to-text system might not be used reliably to provide closed captions for online lectures because it fails to handle technical jargon.
- The authors should discuss the computational efficiency of the proposed algorithms and how they scale with dataset size.
- If applicable, the authors should discuss possible limitations of their approach to address problems of privacy and fairness.
- While the authors might fear that complete honesty about limitations might be used by reviewers as grounds for rejection, a worse outcome might be that reviewers discover limitations that aren't acknowledged in the paper. The authors should use their best judgment and recognize that individual actions in favor of transparency play an important role in developing norms that preserve the integrity of the community. Reviewers will be specifically instructed to not penalize honesty concerning limitations.

3. Theory Assumptions and Proofs

Question: For each theoretical result, does the paper provide the full set of assumptions and a complete (and correct) proof?

Answer: [NA]

Justification: The paper does not include theoretical results.

Guidelines:

- The answer NA means that the paper does not include theoretical results.
- All the theorems, formulas, and proofs in the paper should be numbered and cross-referenced.
- All assumptions should be clearly stated or referenced in the statement of any theorems.
- The proofs can either appear in the main paper or the supplemental material, but if they appear in the supplemental material, the authors are encouraged to provide a short proof sketch to provide intuition.
- Inversely, any informal proof provided in the core of the paper should be complemented by formal proofs provided in appendix or supplemental material.
- Theorems and Lemmas that the proof relies upon should be properly referenced.

4. Experimental Result Reproducibility

Question: Does the paper fully disclose all the information needed to reproduce the main experimental results of the paper to the extent that it affects the main claims and/or conclusions of the paper (regardless of whether the code and data are provided or not)?

Answer: [Yes]

Justification: the paper fully discloses all the information needed to reproduce the main experimental results of the paper to the extent that it affects the main claims and conclusions of the paper.

Guidelines:

- The answer NA means that the paper does not include experiments.
- If the paper includes experiments, a No answer to this question will not be perceived well by the reviewers: Making the paper reproducible is important, regardless of whether the code and data are provided or not.
- If the contribution is a dataset and/or model, the authors should describe the steps taken to make their results reproducible or verifiable.
- Depending on the contribution, reproducibility can be accomplished in various ways. For example, if the contribution is a novel architecture, describing the architecture fully might suffice, or if the contribution is a specific model and empirical evaluation, it may be necessary to either make it possible for others to replicate the model with the same dataset, or provide access to the model. In general, releasing code and data is often one good way to accomplish this, but reproducibility can also be provided via detailed instructions for how to replicate the results, access to a hosted model (e.g., in the case of a large language model), releasing of a model checkpoint, or other means that are appropriate to the research performed.
- While NeurIPS does not require releasing code, the conference does require all submissions to provide some reasonable avenue for reproducibility, which may depend on the nature of the contribution. For example
 - (a) If the contribution is primarily a new algorithm, the paper should make it clear how to reproduce that algorithm.
 - (b) If the contribution is primarily a new model architecture, the paper should describe the architecture clearly and fully.
 - (c) If the contribution is a new model (e.g., a large language model), then there should either be a way to access this model for reproducing the results or a way to reproduce the model (e.g., with an open-source dataset or instructions for how to construct the dataset).
 - (d) We recognize that reproducibility may be tricky in some cases, in which case authors are welcome to describe the particular way they provide for reproducibility. In the case of closed-source models, it may be that access to the model is limited in some way (e.g., to registered users), but it should be possible for other researchers to have some path to reproducing or verifying the results.

5. Open access to data and code

Question: Does the paper provide open access to the data and code, with sufficient instructions to faithfully reproduce the main experimental results, as described in supplemental material?

Answer: [Yes]

Justification: The paper provides open access to the data and code, with sufficient instructions to faithfully reproduce the main experimental results, as described in the supplemental material.

Guidelines:

- The answer NA means that paper does not include experiments requiring code.
- Please see the NeurIPS code and data submission guidelines (<https://nips.cc/public/guides/CodeSubmissionPolicy>) for more details.
- While we encourage the release of code and data, we understand that this might not be possible, so “No” is an acceptable answer. Papers cannot be rejected simply for not including code, unless this is central to the contribution (e.g., for a new open-source benchmark).
- The instructions should contain the exact command and environment needed to run to reproduce the results. See the NeurIPS code and data submission guidelines (<https://nips.cc/public/guides/CodeSubmissionPolicy>) for more details.
- The authors should provide instructions on data access and preparation, including how to access the raw data, preprocessed data, intermediate data, and generated data, etc.
- The authors should provide scripts to reproduce all experimental results for the new proposed method and baselines. If only a subset of experiments are reproducible, they should state which ones are omitted from the script and why.
- At submission time, to preserve anonymity, the authors should release anonymized versions (if applicable).
- Providing as much information as possible in supplemental material (appended to the paper) is recommended, but including URLs to data and code is permitted.

6. Experimental Setting/Details

Question: Does the paper specify all the training and test details (e.g., data splits, hyperparameters, how they were chosen, type of optimizer, etc.) necessary to understand the results?

Answer: [Yes]

Justification: The paper specifies all the details necessary to understand the results in the section A.

Guidelines:

- The answer NA means that the paper does not include experiments.
- The experimental setting should be presented in the core of the paper to a level of detail that is necessary to appreciate the results and make sense of them.
- The full details can be provided either with the code, in appendix, or as supplemental material.

7. Experiment Statistical Significance

Question: Does the paper report error bars suitably and correctly defined or other appropriate information about the statistical significance of the experiments?

Answer: [Yes]

Justification: The paper ensure the reproducibility of the experiment by fixing random seeds.

Guidelines:

- The answer NA means that the paper does not include experiments.
- The authors should answer "Yes" if the results are accompanied by error bars, confidence intervals, or statistical significance tests, at least for the experiments that support the main claims of the paper.

- The factors of variability that the error bars are capturing should be clearly stated (for example, train/test split, initialization, random drawing of some parameter, or overall run with given experimental conditions).
- The method for calculating the error bars should be explained (closed form formula, call to a library function, bootstrap, etc.)
- The assumptions made should be given (e.g., Normally distributed errors).
- It should be clear whether the error bar is the standard deviation or the standard error of the mean.
- It is OK to report 1-sigma error bars, but one should state it. The authors should preferably report a 2-sigma error bar than state that they have a 96% CI, if the hypothesis of Normality of errors is not verified.
- For asymmetric distributions, the authors should be careful not to show in tables or figures symmetric error bars that would yield results that are out of range (e.g. negative error rates).
- If error bars are reported in tables or plots, The authors should explain in the text how they were calculated and reference the corresponding figures or tables in the text.

8. Experiments Compute Resources

Question: For each experiment, does the paper provide sufficient information on the computer resources (type of compute workers, memory, time of execution) needed to reproduce the experiments?

Answer: [Yes]

Justification: The paper provides sufficient information on the computer resources in the section [A](#).

Guidelines:

- The answer NA means that the paper does not include experiments.
- The paper should indicate the type of compute workers CPU or GPU, internal cluster, or cloud provider, including relevant memory and storage.
- The paper should provide the amount of compute required for each of the individual experimental runs as well as estimate the total compute.
- The paper should disclose whether the full research project required more compute than the experiments reported in the paper (e.g., preliminary or failed experiments that didn't make it into the paper).

9. Code Of Ethics

Question: Does the research conducted in the paper conform, in every respect, with the NeurIPS Code of Ethics <https://neurips.cc/public/EthicsGuidelines>?

Answer: [Yes]

Justification: The research conducted in the paper conform, in every respect, with the NeurIPS Code of Ethics.

Guidelines:

- The answer NA means that the authors have not reviewed the NeurIPS Code of Ethics.
- If the authors answer No, they should explain the special circumstances that require a deviation from the Code of Ethics.
- The authors should make sure to preserve anonymity (e.g., if there is a special consideration due to laws or regulations in their jurisdiction).

10. Broader Impacts

Question: Does the paper discuss both potential positive societal impacts and negative societal impacts of the work performed?

Answer: [NA]

Justification: There is no societal impact of the work performed.

Guidelines:

- The answer NA means that there is no societal impact of the work performed.

- If the authors answer NA or No, they should explain why their work has no societal impact or why the paper does not address societal impact.
- Examples of negative societal impacts include potential malicious or unintended uses (e.g., disinformation, generating fake profiles, surveillance), fairness considerations (e.g., deployment of technologies that could make decisions that unfairly impact specific groups), privacy considerations, and security considerations.
- The conference expects that many papers will be foundational research and not tied to particular applications, let alone deployments. However, if there is a direct path to any negative applications, the authors should point it out. For example, it is legitimate to point out that an improvement in the quality of generative models could be used to generate deepfakes for disinformation. On the other hand, it is not needed to point out that a generic algorithm for optimizing neural networks could enable people to train models that generate Deepfakes faster.
- The authors should consider possible harms that could arise when the technology is being used as intended and functioning correctly, harms that could arise when the technology is being used as intended but gives incorrect results, and harms following from (intentional or unintentional) misuse of the technology.
- If there are negative societal impacts, the authors could also discuss possible mitigation strategies (e.g., gated release of models, providing defenses in addition to attacks, mechanisms for monitoring misuse, mechanisms to monitor how a system learns from feedback over time, improving the efficiency and accessibility of ML).

11. Safeguards

Question: Does the paper describe safeguards that have been put in place for responsible release of data or models that have a high risk for misuse (e.g., pretrained language models, image generators, or scraped datasets)?

Answer: [NA]

Justification: The paper poses no such risks.

Guidelines:

- The answer NA means that the paper poses no such risks.
- Released models that have a high risk for misuse or dual-use should be released with necessary safeguards to allow for controlled use of the model, for example by requiring that users adhere to usage guidelines or restrictions to access the model or implementing safety filters.
- Datasets that have been scraped from the Internet could pose safety risks. The authors should describe how they avoided releasing unsafe images.
- We recognize that providing effective safeguards is challenging, and many papers do not require this, but we encourage authors to take this into account and make a best faith effort.

12. Licenses for existing assets

Question: Are the creators or original owners of assets (e.g., code, data, models), used in the paper, properly credited and are the license and terms of use explicitly mentioned and properly respected?

Answer: [Yes]

Justification: The paper cites the original papers of assets used and introduces the details in the section [A](#).

Guidelines:

- The answer NA means that the paper does not use existing assets.
- The authors should cite the original paper that produced the code package or dataset.
- The authors should state which version of the asset is used and, if possible, include a URL.
- The name of the license (e.g., CC-BY 4.0) should be included for each asset.
- For scraped data from a particular source (e.g., website), the copyright and terms of service of that source should be provided.

- If assets are released, the license, copyright information, and terms of use in the package should be provided. For popular datasets, paperswithcode.com/datasets has curated licenses for some datasets. Their licensing guide can help determine the license of a dataset.
- For existing datasets that are re-packaged, both the original license and the license of the derived asset (if it has changed) should be provided.
- If this information is not available online, the authors are encouraged to reach out to the asset's creators.

13. **New Assets**

Question: Are new assets introduced in the paper well documented and is the documentation provided alongside the assets?

Answer: [Yes]

Justification: The details of the new assets are introduced in the section 4 and the section A.

Guidelines:

- The answer NA means that the paper does not release new assets.
- Researchers should communicate the details of the dataset/code/model as part of their submissions via structured templates. This includes details about training, license, limitations, etc.
- The paper should discuss whether and how consent was obtained from people whose asset is used.
- At submission time, remember to anonymize your assets (if applicable). You can either create an anonymized URL or include an anonymized zip file.

14. **Crowdsourcing and Research with Human Subjects**

Question: For crowdsourcing experiments and research with human subjects, does the paper include the full text of instructions given to participants and screenshots, if applicable, as well as details about compensation (if any)?

Answer: [NA]

Justification: The paper does not involve crowdsourcing nor research with human subjects.

Guidelines:

- The answer NA means that the paper does not involve crowdsourcing nor research with human subjects.
- Including this information in the supplemental material is fine, but if the main contribution of the paper involves human subjects, then as much detail as possible should be included in the main paper.
- According to the NeurIPS Code of Ethics, workers involved in data collection, curation, or other labor should be paid at least the minimum wage in the country of the data collector.

15. **Institutional Review Board (IRB) Approvals or Equivalent for Research with Human Subjects**

Question: Does the paper describe potential risks incurred by study participants, whether such risks were disclosed to the subjects, and whether Institutional Review Board (IRB) approvals (or an equivalent approval/review based on the requirements of your country or institution) were obtained?

Answer: [NA]

Justification: The paper does not involve crowdsourcing nor research with human subjects.

Guidelines:

- The answer NA means that the paper does not involve crowdsourcing nor research with human subjects.
- Depending on the country in which research is conducted, IRB approval (or equivalent) may be required for any human subjects research. If you obtained IRB approval, you should clearly state this in the paper.

- We recognize that the procedures for this may vary significantly between institutions and locations, and we expect authors to adhere to the NeurIPS Code of Ethics and the guidelines for their institution.
- For initial submissions, do not include any information that would break anonymity (if applicable), such as the institution conducting the review.